BASIC PROPERTIES OF THE FIELDS EXCITED BY VED AND HMD LOCATED IN A DIELECTRIC SUBSTRATE BACKED BY A PERFECTLY CONDUCTING GROUND PLANE

Natalia Yu. Bliznyuk and Alexander I. Nosich
Institute of Radiophysics and Electronics
National Academy of Sciences
Kharkov 310085, Ukraine

Received 5 March 1997

ABSTRACT: *Fundamental antenna effects of a dielectric substrate backed by a perfectly conducting ground plane and excited by elementary dipoles are studied. The effect of the surface waves and the radiation efficiency as a function of substrate thickness and permittivity are analyzed. © 1997 John Wiley & Sons, Inc.* Microwave Opt Technol Lett 15: 316–320, 1997.

Key words: *dielectric substrate; dipole; surface wave; power; pattern; radiation efficiency*

I. INTRODUCTION

Microstrip structures are now widely used in ground-based and aerospace antenna applications. In this article the fundamental antenna effects of dielectric substrate materials backed by a perfectly electric conducting (PEC) ground plane are investigated. These effects include radiation efficiency, normalized power, and radiation pattern. In order to analyze the basic properties of this canonical substrate fed by a coaxial line or an elementary slot, the problems of the Hertzian vertical electrical dipole (VED) and horizontal magnetic dipole (HMD) are solved analytically. Although similar problems were considered in [1–7], it appears that the mentioned characteristics have been studied only in the case of a horizontal electric dipole placed on top of a dielectric substrate.

At first, the field-potential components for the infinitesimal dipoles are derived with the use of Sommerfeld's method in the form of the Fourier–Bessel integrals. After that, saddle-point integration is used to compute the space-wave radiation pattern, the surface-wave power in the transverse-magnetic (TM) surface waves excited by VED, and the hybrid and transverse-electric (TE) surface waves of HMD. Both parts of the Poynting theorem are used to check the results. Overall antenna parameters are further computed and discussed, and the role of the substrate is found.

II. PROBLEM FORMULATION

The geometry of the problem of VED and HMD located on the substrate-covered PEC ground plane with infinite transverse directions is shown in Figure 1. The origin of the coordinate system is chosen at the dipole. Assuming a time dependence of the form $e^{i\omega t}$, the electromagnetic fields in such a structure can be derived from the vector potentials as

$$\mathbf{E} = -i\omega\mu\mathbf{A}^e + \frac{1}{i\omega\varepsilon}\,\mathrm{grad}\,\mathrm{div}\,\mathbf{A}^e - \mathrm{rot}\,\mathbf{A}^m \tag{1}$$

$$\mathbf{H} = -i\omega\varepsilon\mathbf{A}^m + \frac{1}{i\omega\mu}\,\mathrm{grad}\,\mathrm{div}\,\mathbf{A}^m + \mathrm{rot}\,\mathbf{A}^e \tag{2}$$

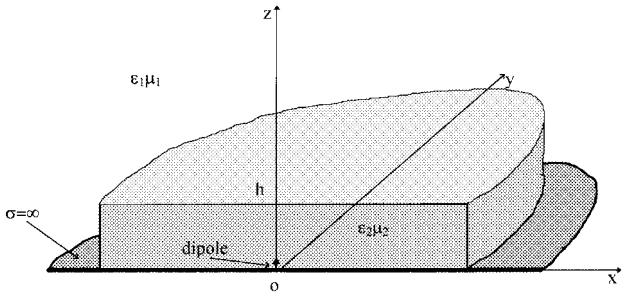

Figure 1 Geometry of the problem

It is known that the vector potentials are tied with the electrical and magnetic currents $\mathbf{J}^{e,m}$ by the following expression:

$$\mathbf{A}^{e,m}(p) = \int_V \mathbf{J}^{e,m}(q)G(p,q)\,dv, \tag{3}$$

where p and q are the observation and source points, respectively, G is the Green's function:

$$G = \frac{1}{8\pi}\sum_{n=-\infty}^{\infty} e^{-in\varphi}\int_{\kappa=-\infty}^{\infty} e^{\pm\gamma(z-z')}\frac{\kappa}{\gamma}J_n(\kappa r')H_n^{(2)}(\kappa r)\,d\kappa, \tag{4}$$

where κ and γ are the radial and vertical components of the wave number:

$$k^2 = \omega^2\varepsilon\mu = \kappa^2 + \gamma^2,$$

and ρ, φ, z are the cylindrical coordinates. The boundary conditions for the tangential field components in the microstrip structure are

$$[\mathbf{n}, \mathbf{E}^2] = 0, \qquad z = 0, \tag{5}$$

$$[\mathbf{n}, \mathbf{E}^1 - \mathbf{E}^2] = 0, \qquad [\mathbf{n}, \mathbf{H}^1 - \mathbf{H}^2] = 0, \qquad z = h, \tag{6}$$

where indices 1 and 2 refer to the air and the dielectric substrate, respectively.

A. Vertical Electrical Dipole. Consider a z-directed VED of the amplitude $I^e l$ located on the dielectric–ground-plane interface:

$$J_z^e = I^e l\frac{\delta(r'-a)}{r}\delta(z'-d)\,\delta(\phi'-0). \tag{7}$$

We split the field into the incident and the scattered fields, and, following the Sommerfeld method [1], introduce an electric vector potential by using (3) and (4). In the case of a z-directed source, in the space domain this potential is given as follows:

$$A_z^{\mathrm{in}} = \frac{I^e l}{8\pi}\int_{-\infty}^{\infty} H_0^{(2)}(\kappa r)\frac{e^{\pm\gamma_2(z-d)}}{\gamma_2}\kappa\,d\kappa. \tag{8}$$

Note that this value differs from the electric-type Hertz potential only by a constant factor. For a VED, no need to consider a magnetic-type vector potential arises. We search for the scattered field potential components in each of two

regions by analogy of the incident field. After satisfying the boundary conditions (5), (6) and assuming that a dipole is located on a ground plane, that is, the potentials are obtained as

$$A_z^1 = \frac{I^e l \varepsilon_1}{4\pi} \int_{-\infty}^{\infty} H_0^{(2)}(\kappa r) \frac{e^{-\gamma_1(z-h)}}{D_m(\kappa)} \kappa \, d\kappa, \tag{9}$$

$$A_z^2 = \frac{I^e l}{4\pi} \int_{-\infty}^{\infty} \frac{\gamma_2 \varepsilon_1 \cosh \gamma_2(z-h) - \gamma_1 \varepsilon_2 \sinh \gamma_2(z-h)}{D_m(\kappa)} \times \frac{H_0^{(2)}(\kappa r)}{\gamma_2} \kappa \, d\kappa, \tag{10}$$

where

$$D_m(\kappa) = \gamma_2 \varepsilon_1 \sinh \gamma_2 h + \gamma_1 \varepsilon_2 \cosh \gamma_2 h. \tag{11}$$

The real zeros of $D_m(\kappa)$ correspond to the TM surface-wave poles of the lossless substrate. Thus, the fields can be found with the aid of (1) and (2) and (9) and (10).

B. Horizontal Magnetic Dipole. The current density of an HMD is given by the following expression:

$$J_x^m = I^m l \frac{\delta(r' - a)}{r} \delta(z' - d) \, \delta(\varphi' - 0). \tag{12}$$

It is well known [6] that two components for the magnetic vector potential A_x^m and A_z^m are needed to satisfy the boundary conditions. The potentials for the incident field are

$$A_x^{\text{in}} = \frac{I^m l}{8\pi} \int_{-\infty}^{\infty} H_0^{(2)}(\kappa r) \frac{e^{\pm \gamma_z z}}{\gamma_2} \kappa \, d\kappa, \tag{13}$$

$$A_z^{\text{in}} = \frac{I^m l}{8\pi} \int_{-\infty}^{\infty} H_1^{(2)}(\kappa r) \frac{e^{\pm \gamma_z z}}{\gamma_2} \kappa \cos \varphi \, d\kappa. \tag{14}$$

As in the case of VED, to satisfy the boundary conditions the potentials in both regions are considered. In the space domain, the total-field potentials, after simplifying and combining some of the terms, are obtained, in the substrate, as

$$A_x^2 = \frac{J^m \, dx}{4\pi} \int_{-\infty}^{\infty} H_0^{(2)}(\kappa \rho) \frac{U(\kappa, z)}{\gamma_2 \, D_m(\kappa)} \kappa \, d\kappa, \tag{15}$$

$$A_z^2 = \frac{J^m \, dx}{8\pi} (\varepsilon_1 - \varepsilon_2) \times \cos \varphi \int_{-\infty}^{\infty} H_1^{(2)}(\kappa \rho) \frac{\sinh[\gamma_2(z+h)]}{D_m(\kappa) \, D_e(\kappa)} \kappa^2 \, d\kappa, \tag{16}$$

and in the air as

$$A_x^1 = \frac{J^m \, dx}{4\pi} \varepsilon_2 \int_{-\infty}^{\infty} H_0^{(2)}(\kappa \rho) \frac{\exp(-\gamma_1 z)}{D_m(\kappa)} \kappa \, d\kappa, \tag{17}$$

$$A_z^1 = \frac{J^m \, dx}{8\pi} (\varepsilon_2 - \varepsilon_1) \times \cos \varphi \int_{-\infty}^{\infty} H_1^{(2)}(\kappa \rho) \frac{\sinh(\gamma_2 h) \exp(-\gamma_1 z)}{D_m(\kappa) \, D_e(\kappa)} \kappa^2 \, d\kappa, \tag{18}$$

where

$$D_e(\kappa) = \gamma_1 \sinh(\gamma_2 h) + \gamma_2 \cosh(\gamma_2 h), \tag{19}$$

$$U(\kappa) = \gamma_2 \varepsilon_1 \cosh(\gamma_2 z) - \gamma_1 \varepsilon_2 \sinh(\gamma_2 z). \tag{20}$$

The real zeros of $D_m(\kappa)$ and $D_e(\kappa)$ give the wave numbers of the characteristic hybrid surface-wave modes propagating in such a structure. As might be expected, the A_z components vanishes when the substrate is absent.

III. APPLICATION OF THE POYNTING THEOREM

The Poynting theorem in the complex form (with real parts defining the time-average power values) can be used to obtain a partial validation of the obtained results:

$$-\tfrac{1}{2} \operatorname{Re} \int_V \left(\mathbf{j}^e \mathbf{E} + j^m \dot{\mathbf{H}} \right) dv = \operatorname{Re} \int_S \mathbf{P} \times \mathbf{n} \, ds, \tag{21}$$

where $\mathbf{P} = \frac{1}{2}[\mathbf{E}, \mathbf{H}^*]$ is the Poynting vector, and S is a surface enclosing a finite volume V. We choose S as a finite-height circular-cylindrical surface capped with a spherical roof, with the radii and the height expanding to infinity. Then the right-hand part can be simplified by the use of the far-field expressions reduced to the contour integration in the complex κ plane:

$$\int_{-\infty}^{\infty} F(\kappa) \, d\kappa = \int_{\Omega} F(\kappa) \, d\kappa + \int_{\Gamma_\infty} F(\kappa) \, d\kappa + 2\pi i \sum_m \operatorname{res} F(\kappa_m). \tag{22}$$

The integration contour is to be shifted under the κ axis to bypass the poles and the cuts. The integral along the infinitely remote contour Γ_∞ vanishes. The branch-cut integral along the cut Q can be estimated by the saddle-point method [2] and yields a spherical wave. The surface wave fields are determined by computing the residues at the poles located in the interval $[1, \sqrt{\varepsilon_2 \mu_2}]$ of the real axis. The surface-wave powers are obtained by integrating the radial component of the Poynting vector over a circular cylindrical surface. The space-wave power is obtained by integrating the spherical wave of the Poynting vector over the spherical surface.

The left-hand-part integration, which takes account of (7) or (12), is reduced to the corresponding total field component taken at the source point. The powers of the surface and the space waves are then obtained similarly via the contour integration in the complex κ plane. The resulting surface-wave power expressions are the same as the ones obtained with the use of the right-hand part of (21). The space-wave power (real part) is reduced to the definite integral, over the interval $[-\sqrt{\varepsilon_2 \mu_2}, \sqrt{\varepsilon_2 \mu_2}]$. After some algebra, it can be converted to the form obtained previously.

IV. NUMERICAL RESULTS

In the computations all of the power characteristics were normalized to the radiation power of a dipole located on the PEC ground plane in free space:

$$P_{\text{norm}} = \frac{(I^{e,m} l k_1)^2}{6\pi} \sqrt{\frac{\varepsilon_1}{\mu_1}}. \tag{23}$$

A. Surface-Wave Power. The total surface-wave power is the sum of the powers carried by each wave, because these are

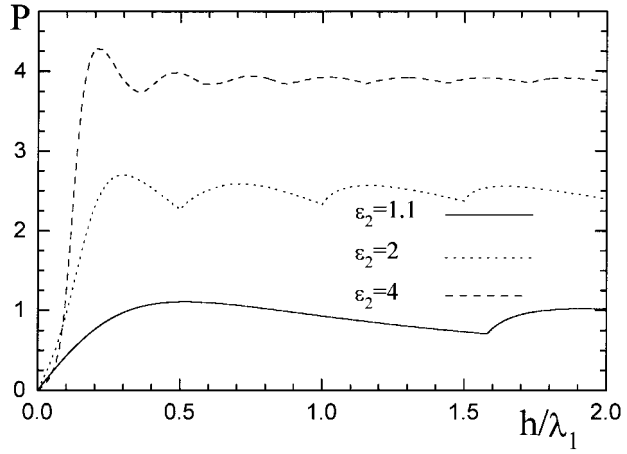

Figure 2 The total surface wave power—VED case

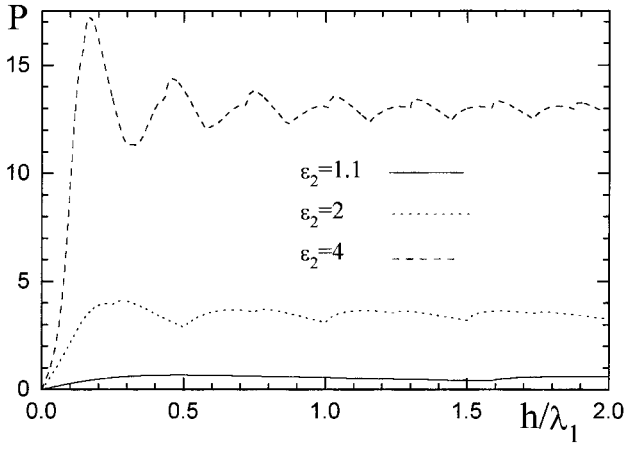

Figure 3 The total surface-wave power—HMD case

orthogonal [5]. Figures 2 and 3 show this quantity for the different media, as a function of the substrate thickness, for VED and HMD cases, respectively. As is seen, a flat-layer dielectric substrate is a good waveguide for the surface waves. If the substrate thickness increases, the total surface-wave power becomes quickly larger than unity. Here, the power of the individual modes rises and falls but the total power is oscillating with a damping amplitude. But in the case of a HMD the surface-wave power is larger than for a VED.

B. Radiation Pattern. The radiation patterns for different dipoles are plotted in the Figures 4 and 5. One can see that the dependence of VED and HMD patterns versus the substrate thickness is the same: As the thickness increases, the number of lobes increases as well. But as the permittivities of the substrate increase, the power of VED radiation decreases, unlike the HMD case. This effect can be explained by the distinctions between the structures of the fields of VED and HMD.

C. Space Wave Power. Figures 6 and 7 show the behavior of the space-wave power versus the substrate thickness. These curves have two principally different basic features: periodic oscillations caused by varying electrical thickness of the substrate, and peaks appearing with a different period, at the points where a new surface wave is able to propagate (at the

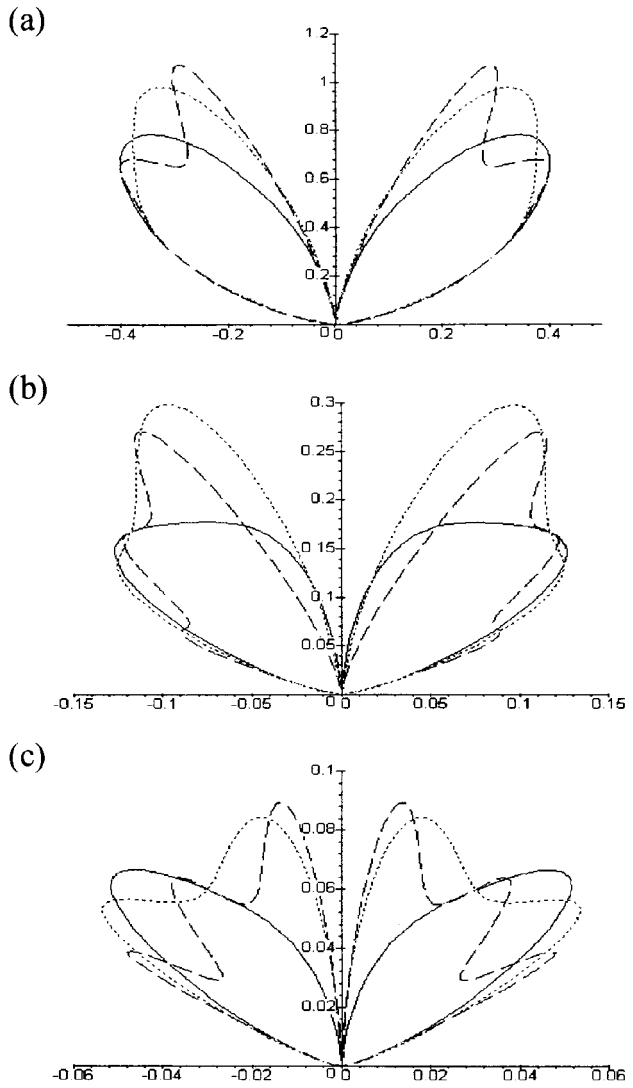

Figure 4 The radiation pattern of VED. (a) $\varepsilon_2 = 1.1$, (b) $\varepsilon_2 = 2$, (c) $\varepsilon_2 = 4$. Solid lines, $h/\lambda_2 = 0.75$; dotted lines, $h/\lambda_2 = 1$; dashed lines, $h/\lambda_2 = 2.3$

cutoff frequencies—see Figures 8 and 9). As far as we know, the latter effect has not been studied before. In fact, this is a threshold phenomenon, closely related to the so-called Wood's anomalies of periodic gratings and closed waveguides.

As seen in Figure 9, for the HMD case the powers of the hybrid modes are greater than the powers of TE modes. In addition, the space-wave power increases with increasing substrate permittivity for HMD, unlike the VED, case where it decreases.

D. Radiation Efficiency. The radiation efficiency of the microstrip antenna on a lossless substrate is defined as

$$\eta = \frac{P_{\text{sp}}}{P_{\text{sur}} + P_{\text{sp}}}. \tag{24}$$

In Figures 10 and 11, the curves of the radiation efficiency versus the substrate thickness for different media are plotted for VED and HMD, respectively. In each case, a maximum radiation efficiency is obtained either at the cutoff frequency

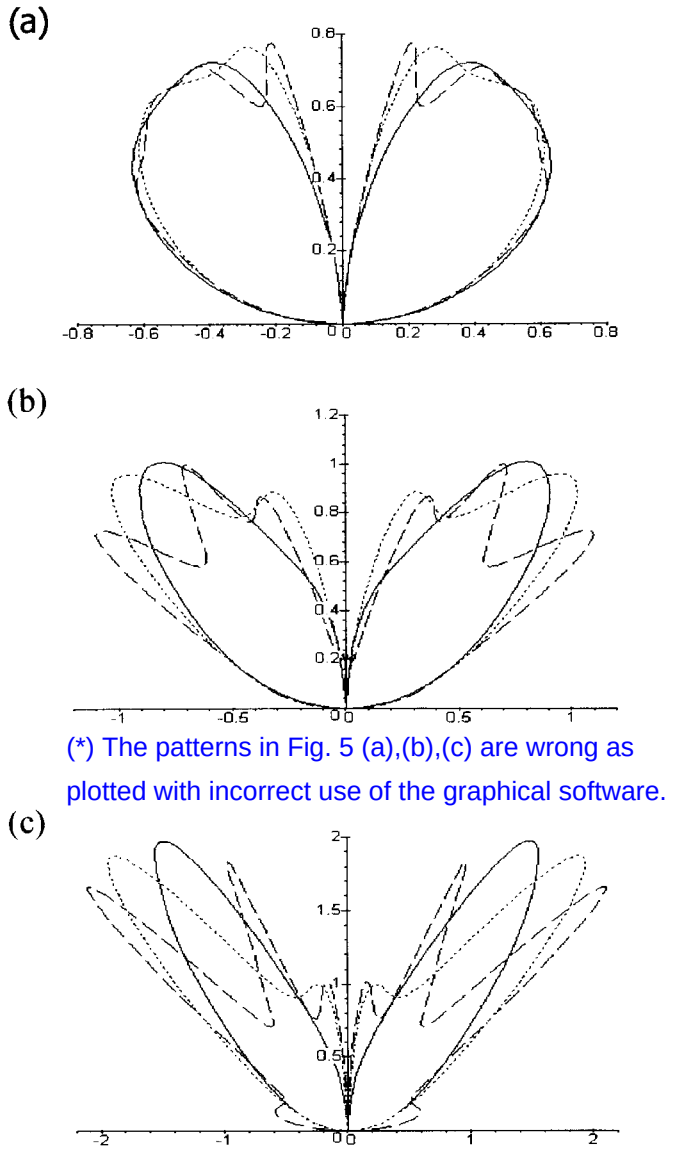

(*) The patterns in Fig. 5 (a),(b),(c) are wrong as plotted with incorrect use of the graphical software.

Figure 5 The radiation pattern of HMD. (a) $\varepsilon_2 = 1.1$, (b) $\varepsilon_2 = 2$, (c) $\varepsilon_2 = 4$. Solid lines, $h/\lambda_2 = 0.75$; dotted lines, $h/\lambda_2 = 1$; dashed lines, $h/\lambda_2 = 2.3$ see (*); correct patterns show maximum radiation at the normal direction

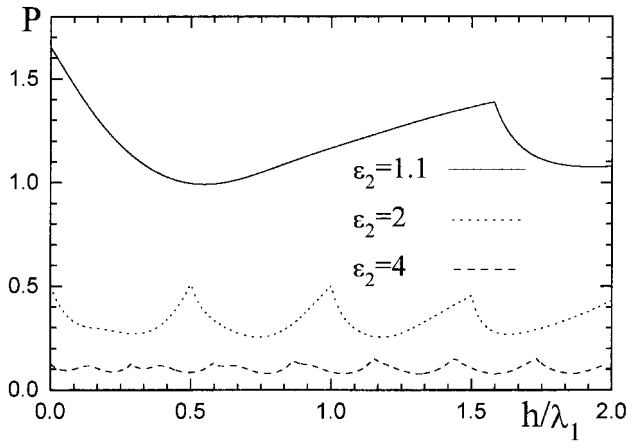

Figure 6 The space-wave power—VED case

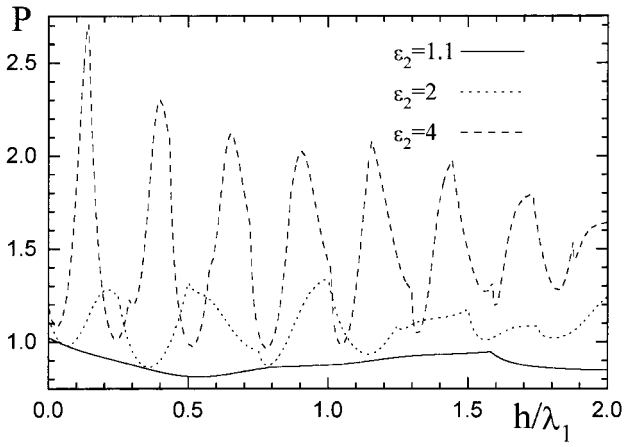

Figure 7 The space-wave power—HMD case

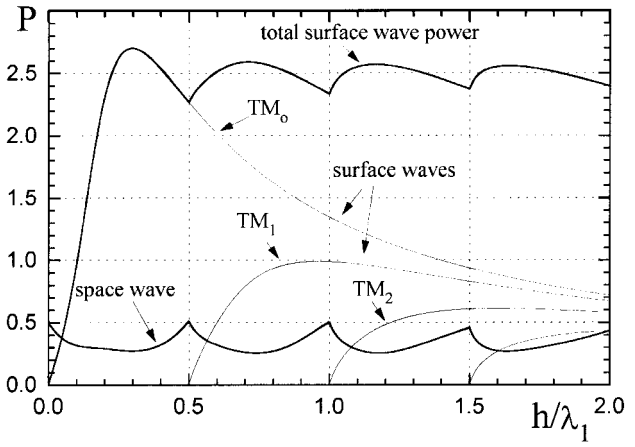

Figure 8 The surface-wave power and the space wave power versus substrate thickness ($\varepsilon_2 = 2$, VED)

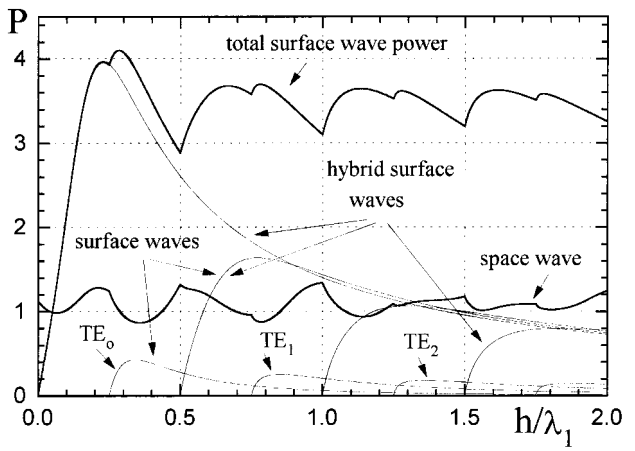

Figure 9 The surface-wave power and the space-wave power versus substrate thickness ($\varepsilon_2 = 2$, HMD)

of a surface mode or at the frequency of an interference peak (see Figures 6 and 7). The greater the dielectric constant, the lower the average value of the radiation efficiency, the greater the amplitude of the interference oscillations, and the smaller the period of the latter.

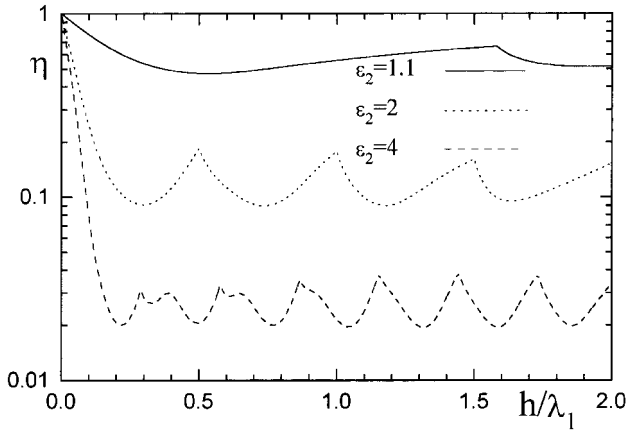

Figure 10 The radiation efficiency—VED case

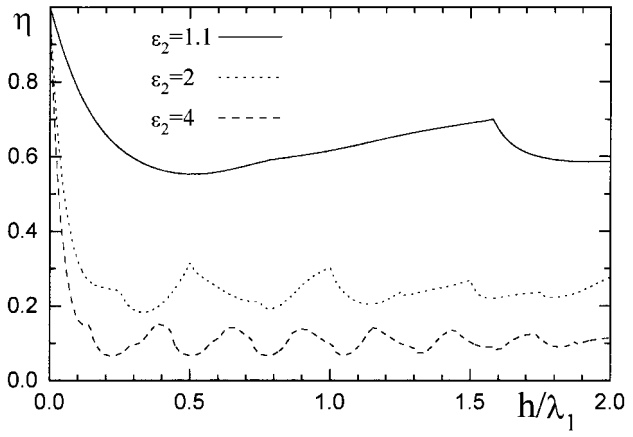

Figure 11 The radiation efficiency—HMD case

V. CONCLUSIONS

In this article the effect of the grounded substrate on the radiation of VED and HMD has been considered. To validate the results we have used the Poynting theorem. It is found that the radiation efficiency is reduced because of the surface-wave excitation. The space-wave power has periodic oscillations caused by varying the electrical thickness of the substrate, and generally smaller but sharper peaks at the points where a new surface wave is able to propagate. The space-wave power increases with increasing substrate permittivity for HMD, unlike the VED case, where it decreases.

The surface-wave powers in the HMD case are greater than the surface-wave powers in the VED case. For the both kinds of excitation, the radiation efficiency decreases with increasing substrate permittivity, and is greater in the HMD case.

It is hoped that the above-presented analysis will serve as reference data in the further research on the radiation of disk-patch antennas and arrays fed by VED and HMD.

ACKNOWLEDGMENTS

The authors are grateful to Professor F. Gardiol for discussion and encouragement, and to the IEEE MTT Society for the support through a graduate fellowship award.

REFERENCES

1. G. T. Markov and A. F. Chaplin, *Excitation of Electromagnetic Waves*, Energiya Publ., Moscow, 1967 (in Russian).
2. B. Felsen and N. Marcuvitz, *Radiation and Scattering of Waves*, Prentice-Hall, Englewood Cliffs, NJ, 1973.
3. N. G. Alexopoulos, P. B. Katehi, and D. B. Rutledge, "Substrate Optimisation for Integrated Circuit Antennas," *IEEE Trans. Microwave Theory Tech.*, Vol. MTT-31, No. 7, 1983, pp. 550–557.
4. N. G. Alexopoulos and D. R. Jackson, "Fundamental Superstrate (Cover) Effects on Printed Circuit Antennas," *IEEE Trans. Antennas Propagat.*, Vol. AP-32, No. 8, 1984, pp. 807–816.
5. D. R. Jackson and N. G. Alexopoulos, "Microstrip Dipoles on Electrically Thick Substrates," *Int. J. Infrared Millimeter Waves*, Vol. 7, No. 1, 1986, pp. 1–26.
6. J. R. Mosig and T. K. Sarkar, "Comparison of Quasi-Static and Exact Electromagnetic Fields from a Horizontal Electric Dipole above a Lossy Dielectric Backed by an Imperfect Ground Plane," *IEEE Trans. Microwave Theory Tech.*, Vol. MTT-34, No. 4, 1986, pp. 379–387.
7. J. R. Mosig, R. C. Hall, and F. E. Gardiol, "Numerical Analysis of Microstrip Patch Antennas, in J. R. James and P. S. Hall (Eds.), *Handbook of Microstrip Antennas*, Peter Peregrinus, London, 1989, pp. 391–453.

CCC 0895-2477/97

ITERATIVE BOUNDARY CONDITION (IBC) FOR SCATTERING PROBLEMS FROM THE TWO-POINT FIELD EQUATION (2PFE)

Yong-Lun Luo and Kwai-Man Luk
Department of Electronic Engineering
City University of Hong Kong
83 Tat Avenue
Kowloon, Hong Kong

Received 3 January 1997; revised 19 March 1997

ABSTRACT: *The truncation boundary condition is a stumbling block in solving electromagnetic scattering problems by the finite-difference (FD) or finite-element (FE) methods. A simple, exact, and proper boundary condition is always desirable for use in terminating the FD mesh. In this article a novel iterative boundary condition (IBC) is proposed for solving electromagnetic scattering problems by the FD method. This novel boundary condition, expressed by an exact two-point field equation (2PFE) and derived from rigorous analysis of the scattered field or the radiation field, is obtained by an iteration process. The validation of the IBC and the convergence of the iteration processes have been numerically studied. A number of two-dimensional (2D) scattering problems have been successfully solved with IBC. The results agree very well with that obtained by the MoM and the MEI. This novel approach is simple in concept and easy to apply. It can possibly be extended to three-dimensional problems. © 1997 John Wiley & Sons, Inc.* Microwave Opt Technol Lett 15: 320–328, 1997.

Key words: *scattering; finite difference; numerical method*

I. INTRODUCTION

FD and FE are two of the basic methods used to solve electromagnetic wave propagation problems. By FD or FE, the unbounded spatial domain needs to be truncated by an artificial boundary to render the computational domain finite, and a boundary condition must be addressed for the trunca-